

Finite-Temperature Signatures of Spin Liquids in Frustrated Hubbard Model

Takahiro Misawa¹ and Youhei Yamaji^{2,3}

¹*Institute for Solid State Physics, The University of Tokyo,
5-1-5 Kashiwanoha, Kashiwa, Chiba 277-8581, Japan*

²*Quantum-Phase Electronics Center (QPEC), The University of Tokyo,
Hongo, Bunkyo-ku, Tokyo, 113-8656, Japan and*

³*JST, PRESTO, Hongo, Bunkyo-ku, Tokyo, 113-8656, Japan*

(Dated: December 22, 2017)

Finite-temperature properties of the frustrated Hubbard model are theoretically examined by using the recently proposed thermal pure quantum state, which is an unbiased numerical method for finite-temperature calculations. By performing systematic calculations for the frustrated Hubbard model, we show that the geometrical frustration controls the characteristic energy scale of the metal-insulator transitions. We also find that entropy remains large even at moderately high temperature around the region where the quantum spin liquid is expected to appear at zero temperature. We propose that this is a useful criterion whether the target systems have a chance to be the quantum spin liquid or the non-magnetic insulator at zero temperature.

Introduction.— Strong correlations among particles often induce localization of the particles and resultant charge-gapped states are called Mott insulators. The Mott insulators have been ubiquitously found in a broad range of condensed matter physics [1–3]. In most of the Mott insulators in solids, time-reversal symmetry-broken phases such as antiferromagnetic phases appear at sufficiently low temperatures. However, if geometrical frustration becomes large [4], the quantum melting of the magnetic orders leads to new states of matter such as quantum spin liquids (QSL) [5, 6]. Actually, in the several organic conductors, it has been pointed out that QSL appear [7–9]. It has been one of the hottest issues of the modern condensed matter physics to clarify how the interplay of strong electronic correlations and the geometrical frustrations induces the QSL [10].

The two-dimensional Hubbard model with geometrical frustrations, which has the nearest-neighbor [nn] (next-nearest-neighbor [nnn]) hopping t (t') and on-site Coulomb interaction U (details are defined in Eq. (1) later) is one of the simplest theoretical model that describes interplay between the strong electronic correlations and the geometrical frustrations. In this model, due to t' , which induces the nnn antiferromagnetic interactions, as illustrated in the inset of Fig. 1, the competition between two magnetic phases occurs: a simple Néel state becomes stable for small t' while a stripe state becomes stable for large t' region ($t'/t \sim 1$). Several theoretical calculations for the ground states of the frustrated Hubbard model [11–13] and its strong coupling limit J_1 - J_2 Heisenberg model ($J_1 \sim 4t^2/U$, $J_2 \sim 4t'^2/U$) [14–17] have been done thus far and most of the calculations suggest that QSL states appear around the intermediate region. In spite of the huge amount of the studies on the frustrated Hubbard model and J_1 - J_2 Heisenberg model, there are few unbiased theoretical studies on the finite-temperature properties that are accessible in experiments because of a lack of efficient theoretical methods.

In this Letter, by using an efficient unbiased numerical method, i.e., the thermal pure quantum (TPQ) method [18], we systematically study finite-temperature properties of the frustrated Hubbard model, which is a prototypical system where the competition between the geometrical frustrations and the strong electronic correlations plays a crucial role. From the unbiased and systematic calculations, we clarify how the geometrical frustrations controls the crossover temperatures of the Mott transitions and find the finite-temperature signatures of QSL. We also propose an experimental criterion of closeness to the spin liquid phase: Finite-temperature entropy at moderately high temperatures significantly correlates with closeness to the spin liquid phase. Experimental searches for spin liquids have so far focused on setting up an *alibi* of spontaneous symmetry breakings down to ultra-low temperatures. However, we reveal that, even at moderately high temperatures $T \sim t/10$, it becomes clear whether the target system has chance to be a spin liquid at zero temperature.

Model and Methods.— We study the t - t' Hubbard model on a square lattice (see Fig. 1) defined as

$$\hat{\mathcal{H}} = -t \sum_{\langle i,j \rangle, \sigma} (c_{i\sigma}^\dagger c_{j\sigma} + \text{h.c.}) - t' \sum_{\langle\langle i,j \rangle\rangle, \sigma} (c_{i\sigma}^\dagger c_{j\sigma} + \text{h.c.}) + U \sum_i n_{i\uparrow} n_{i\downarrow}, \quad (1)$$

where $c_{i\sigma}^\dagger$ ($c_{i\sigma}$) is a creation (annihilation) operator of an electron with spin σ at i th site. The first (second) term describes the hopping of electrons between the nn (nnn) sites $\langle i, j \rangle$ ($\langle\langle i, j \rangle\rangle$) on the square lattice, and the third term represents the onsite Coulomb interactions ($U > 0$). In the following, we focus on the half filling, i.e., the filling is given by $n = N_s^{-1} \sum_{i\sigma} \langle c_{i\sigma}^\dagger c_{i\sigma} \rangle = 1$ ($N_s = L \times L$ is the system size). To reduce the numerical cost, we only consider the total $S^z = 0$ space, i.e., $S_{\text{total}}^z = \sum_i S_i^z = 0$. We employ a 4×4 cluster with a periodic boundary condition in the most of the present Letter [19].

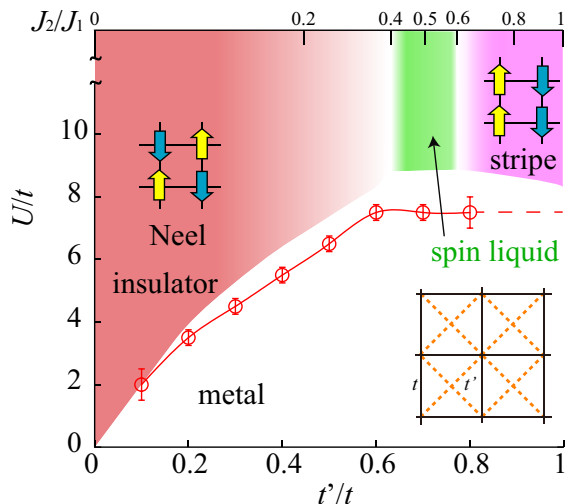


FIG. 1: (color online). Phase diagram for frustrated Hubbard model in comparison with strong-coupling-limit phase diagram. The phase boundary separating insulating and metallic ground states is determined by maxima of χ_D (see main article) as a function of on-site Coulomb repulsion U . Spin liquid may appear between Néel and stripe magnetic orders in the strong coupling region. In the inset, lattice structure used in this study is shown. The nearest-neighbor hopping (next-nearest-neighbor) hopping is represented by t (t').

In the TPQ method [18], by multiplying $(l - \hat{H}/N_s)$ to random vector $|\psi_{\text{rand}}\rangle$, we numerically generate the TPQ state. Here, l is constant that is larger than the maximum eigenvalue of \hat{H}/N_s . The k th TPQ state is recursively defined as $|\psi_k\rangle \equiv (l - \hat{H}/N_s)|\psi_{k-1}\rangle / |(l - \hat{H}/N_s)|\psi_{k-1}\rangle|$ with $|\psi_0\rangle = |\psi_{\text{rand}}\rangle$. It is shown that the temperature T_k corresponding to the k th TPQ state is estimated from the k th internal energy $u_k = \langle \psi_k | \hat{H} | \psi_k \rangle / N_s$ within the accuracy of $O(1/N_s)$, as $\beta_k = 1/k_B T_k = 2k/N_s(l - u_k) + O(1/N_s)$, where k_B is the Boltzmann constant and we take $k_B = 1$ in this Letter. It is shown that physical properties at $T = T_k$ can be calculated as the expectation value taken with respect to $|\psi_k\rangle$, i.e., $\langle \hat{A} \rangle_{T=T_k} = \langle \psi_k | \hat{A} | \psi_k \rangle + O(1/N_s)$. To estimate the finite-size error, we typically perform five runs initiated with different $|\psi_{\text{rand}}\rangle$ and regard its standard deviations as error bars. Here, note that, in the pioneering works [20–22], the finite-temperature observables were already calculated by replacing ensemble average with random sampling of wave functions.

Finite-temperature physical quantities in Hubbard models.— We first show the results of the finite- T calculations for $t'/t = 0.5$ as an example of weakly frustrated Hubbard models. The ground state is expected to be Néel state for $t'/t = 0.5$. Figure 2 (a) shows that temperature dependence of the specific heat C/N_s , which is given by $C/N_s = (\langle \hat{H}^2 \rangle - \langle \hat{H} \rangle^2) / (N_s T^2)$. The specific heat has a single peak for $U/t = 4$ as a function of T while double-peak structures [23] are universal at strong-coupling regions

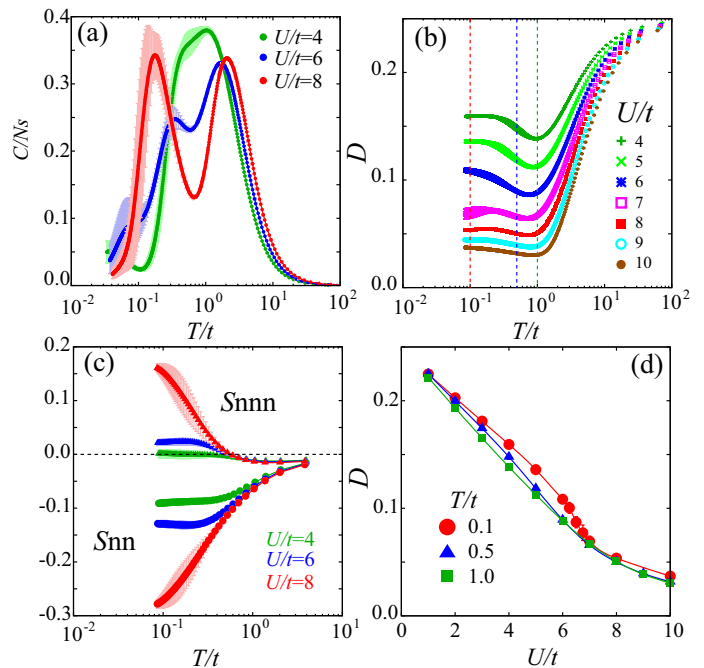


FIG. 2: (color online). (a) Temperature dependence of the specific heat. Error bars are shown as shaded regions. (b) Temperature dependence of double occupancy D for several U . Irrespective of interaction strength, we find the non-monotonic temperature dependence of D . (c) Temperature dependence of the nn (nnn) spin correlation S_{nn} (S_{nnn}), which are defined as $S_p = 1/(z_p N_s) \sum_{i=1}^{N_s} \sum_{\mu} \mathbf{S}_i \cdot \mathbf{S}_{i+e_{\mu}}$, where $p = \text{nn}$ or nnn and accordingly, e_{μ} runs over nn or nnn sites, and z_p represents the coordination number for nn or nnn sites. (d) Interaction (U) dependence of D for $T/t = 1.0, 0.5, 0.1$. By lowering temperature, we can see the signature of the finite-temperature Mott transition.

of the Hubbard-type models irrespective of dimensionality [24–27].

The high-temperature peak of C is generated by the charge degrees of freedom [23, 28] whose energy scale is determined by U , as confirmed later by the peak temperatures insensitive to t' shown in Fig. 4(c). Below the peak temperature, the Mott gap opens and charge degrees of freedom begin to freeze. In other words, below the peak temperature, electrons begin to feel the on-site repulsion U and double occupancy, which is measured by $D = N_s^{-1} \sum_{i=1, N_s} \langle n_{i\uparrow} n_{i\downarrow} \rangle$, is gradually prohibited.

We show temperature dependence of the double occupancy in Fig. 2 (b). Our simulation shows non-monotonic temperature dependence of D from weak to strong coupling region, i.e., D has the minimum around $T/t \sim 1$. We note that this non-monotonic behavior is universal one and observed in a wide range of Hubbard-type models [29–32]. The non-monotonic temperature dependence is explained by the development of antiferromagnetic correlations. Because the antiferromagnetic correlations in-

duce singlet states that have larger double occupancies compared to the other states, the double occupancy increases at low temperature.

The low-temperature peak of the specific heat, in contrast to the high-temperature peak, is induced by spin degrees of freedom [23–27]. This signals development of antiferromagnetic correlations as shown in Fig. 2 (c), which corresponds to an increase in D at low temperatures as discussed above. The peak temperature becomes lower as U increases, as is manifest in Fig. 2 (a), which is consistent with the characteristic energy scale of the spin-degrees of freedom at the strong coupling limit given by the effective superexchange $J_1 \sim 4t^2/U$. To examine the energy scale, we show the temperature dependence of the nn and nnn spin correlations in Fig. 2 (c). As it is expected, the spin correlations develop around the low-temperature peak of the specific heat. The two emergent energy scales corresponding to spin and charge degrees of freedom in the strong coupling region are indeed identified as origin of two-peak structure of the specific heat for $U/t \gtrsim 6$ while separation of these energy scales may not be clear in excitation spectra [33].

Effect of geometrical frustration on metal-insulator transitions.— To examine the signature of the finite-temperature Mott transitions, we calculate the U -dependence of D for several temperatures as shown in Fig. 2 (d). By lowering the temperatures, we find the slope of D becomes steep. Since the slope of D diverges at the finite-temperature Mott critical end point [34], this behavior can be regarded as the crossover of the finite-temperature Mott critical point.

To see the t' dependence of the critical temperatures of the Mott transitions from the crossover behaviors at fixed temperature, we calculate the U dependence of D for sev-

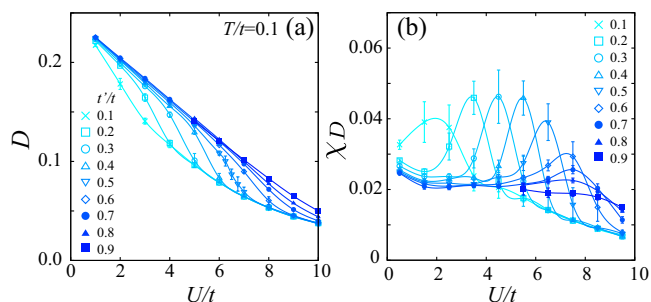


FIG. 3: (color online). (a) Interaction dependence of double occupancy D for several t' at $T/t = 0.1$. The crossover interaction becomes larger by increasing frustration. (b) Interaction dependence of double occupancy susceptibility χ_D for several t' . To reduce the numerical error in numerical differentiation, we take finite difference $\Delta U = 1$. We see the height of peak in χ_D becomes smaller by increasing t' . This result indicates that the critical temperature of Mott critical end point becomes lower by increasing t' . Solid curves are guides for eyes.

eral different t' at $T/t = 0.1$ as shown in Fig. 3 (a). From this data, by performing the numerical differentiation for D with respect to U , we obtain doublon susceptibility $\chi_D = -\partial D/\partial U$. Here, note that, even at zero temperature, the maxima of χ_D as the function of U/t have been demonstrated to signal the Mott transitions in the finite-size Hubbard models [35]. The obtained χ_D is shown in Fig. 3(b). By increasing t' (increasing frustration), we find that the peak values of χ_D at fixed temperature decrease and the peak almost vanishes around $t'/t \sim 0.75$. This result indicates that the critical temperature of the critical end point of the Mott transitions becomes lower by increasing the frustration and the marginal quantum critical point (MQCP) [36, 37] exists around $t'/t \sim 0.75$, where the critical temperature of the Mott transition becomes zero. Because of the limitation of the available system size, it is hard to make a conclusion to the fate of the finite-temperature Mott critical point. However, our results are qualitatively consistent with the mean-field calculations [37, 38] and it is plausible that the MQCP appears around $t'/t \sim 0.75$. We note that ground-state calculations for the Hubbard model on the anisotropic triangular lattice also indicate that nature of Mott transitions is governed by the geometrical frustrations [36, 39].

Signatures of QSL.— Here, to examine the signature of the spin liquid state, we calculate spin correlations for several different t' . As shown in Fig. 4(a) and (b), in the small t' ($t' \lesssim 0.6$), by lowering the temperature, antiferromagnetic nn spin correlations develop while the ferromagnetic nnn spin correlations develop. These spin correlations are consistent with the Néel order. In contrast to this, for large t' region ($t'/t \gtrsim 0.8$), while the antiferromagnetic nnn spin correlations develop, the nn spin correlations remain small even at low temperatures below $t/10$. These spin correlations indicate that the stripe antiferromagnetic order becomes stable in the large t' region. Sandwiched by the Néel and the stripe orders, S_{nnn} is saturated and remains small even at low temperatures for the intermediate t' . We note that short-range spin correlations at moderately high temperatures ($T/t \sim 0.1$) reflect the corresponding ground states and the behavior at $t'/t = 0.75$ is consistent with that of the QSL.

We next examine the thermodynamic properties of the spin-liquid candidates. In contrast to the high-temperature peaks of C insensitive to t' shown in Fig. 4(c), the positions of the second peak largely depend on t' since they are governed by the spin degrees of freedom. At the highly frustrated parameter region $t'/t \sim 0.75$, the amplitude of the second peak remains small and indicates the substantial amount of low-energy excitations is left even below the energy scale $T/t \sim 0.05$.

To quantify the amount of the low-energy excitations, we calculate the entropy. We show temperature dependence of S_{norm} in Fig 4(d). At the highly frustrated region ($t'/t = 0.75$), the entropy is not released down to $T/t \sim 0.05$ compared to weakly frustrated regions.

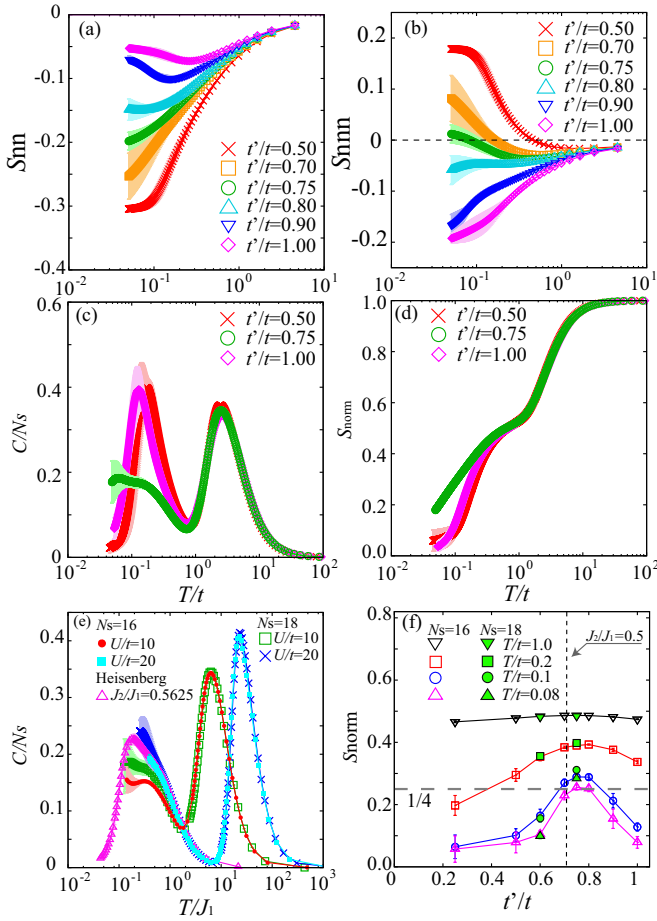


FIG. 4: (color online). (a),(b) Temperature dependence of nearest-neighbor (S_{nn}) and next-nearest-neighbor (S_{nnn}) spin correlations for several different t' at $U/t = 10$. Around $t' \sim 0.75$, S_{nnn} becomes almost zero at low temperature. (c) Temperature dependence of the specific heat for several t' at $U/t = 10$. (d) Temperature dependence of the normalized entropy, which is defined by $S(T)/N_s = c \ln 2 - 1/N_s \int_{-\infty}^T C/T dT$, $S_{norm} = S/(c \ln 2)$, where constant c is 2 if S_{total}^z is unrestricted. In this calculation, we set $S_{total}^z = 0$. Then, c is given by $c = \ln(16 C_8)^2 / 16 \ln 2 \sim 1.706$ for 16 sites. If we take the thermodynamic limit, c converges to 2. For $t'/t \sim 0.75$, large residual entropy is observed compared to $t'/t = 0.5, 1.0$. (e) Temperature dependence of the specific heat of the 4×4 and $3\sqrt{2} \times 3\sqrt{2}$ Hubbard clusters for $t' = 0.75$ at $U/t = 10$ and 20 compared with a $4\sqrt{2} \times 4\sqrt{2}$ Heisenberg cluster [19] by setting $J_1 = 4t^2/U$ and $J_2 = 4t'^2/U$. (f) Frustration (t'/t) dependence of the entropy for several fixed temperatures. Around $t'/t \sim 0.75$, the large remaining entropy is observed and it is the evidence of QSL.

To examine the finite-size effects, we show the specific heat of the 18-site cluster compared with that for the larger U/t and the strong coupling limit [19] in Fig. 4(e) by setting $J_1 = 4t^2/U$ and $J_2 = 4t'^2/U$, at the highly frustrated parameter $t'/t = 0.75$. Although small system size dependence exists, all the data consistently shows

that the reduction of the low-temperature-peak height occurs at $t'/t = 0.75$ compared to the region where the magnetic long-range orders appear.

We also show t' dependence of the entropy at several fixed temperatures in Fig. 4(f). We find that the entropy at fixed temperature has peak around $t'/t \sim 0.75$, where the spin-liquid or non-magnetic ground states are expected at the strong coupling limit [16, 17]. In sharp contrast, for the Néel and stripe order, the entropy quickly becomes zero by decreasing the temperature, which indicates that almost all the degrees of freedom including spin degrees of freedom is released below $T \sim t/10$.

Even at the moderately high temperatures $T \sim t/10$, therefore, the entropy clearly shows whether the target systems have chance to be spin-liquid states at zero temperature. This fact is seemingly trivial since, in the presence of the geometrical frustrations, entropy is expected to remain finite at low temperatures well below the exchange coupling J_1 . However, the present result offers the first unbiased and quantitative criterion for the emergence of the spin-liquid ground states in the geometrically frustrated Mott insulators. Although competition among quantum phases is also expected to show remaining entropy, there are counterexamples. An example is the quantum phase transition from the Kitaev spin liquid [40] to ordered states [41]. When the ground state changes from the spin liquid to an ordered state, entropy at a temperature equal to, for example, one-quarter of the dominant energy scale monotonically decreases and does not show any enhancement above the transition point [42].

In summary, we apply the TPQ method to the frustrated Hubbard model. By calculating the susceptibilities of the double occupancy, we find that the characteristic energy scale of the Mott transition becomes lower by increasing t' . This result indicates emergence of the MQCP around $t'/t \sim 0.75$. We note that the MQCP and QSL appear around nearly the same parameter region and we expect that this coincide is not accidental one: Since infinitesimally small antiferromagnetic order parameters cannot generate a single-particle gap on the entire Fermi surface, another exotic phases such as the QSL are expected to appear [43, 44] in between the paramagnetic metal and the antiferromagnetic insulator if the metal-insulator transition is continuous. We note that it is unlikely but not excluded that the antiferromagnetic metal appears as the intermediate phase as in the mean-field calculations [37, 38]. It is an intriguing issue left for future studies to examine whether the QSL universally appears around the continuous metal insulator transitions including MQCP or not. We also find that large entropy remains at $T/t \sim 0.1$ around the spin-liquid region and this may be useful criterion for searching the QSL. We note that the suppression of magnetic orders due to the low dimensionality [45] and impurities [46], instead of the geometrical frustration, do not induces the large remaining entropy. For the spin liquid candidates,

it is an intriguing challenge to examine whether the proposal will work.

The authors thank Masatoshi Imada for fruitful discussions and comments. A part of calculations is done by using open-source software $\text{H}\Phi$ [47–49]. Our calculation was partly carried out at the Supercomputer Center, Institute for Solid State Physics, University of Tokyo. This work was supported by JSPS KAKENHI (Grant Nos. 15K17702, 16K17746, and 16H06345) and was supported by PRESTO, JST. This work was also supported in part by MEXT as a social and scientific priority issue (Creation of new functional devices and high-performance materials to support next-generation industries) to be tackled by using post-K computer. TM was supported by Building of Consortia for the Development of Human Resources in Science and Technology from the MEXT of Japan.

-
- [1] M. Imada, A. Fujimori, and Y. Tokura, *Rev. Mod. Phys.* **70**, 1039 (1998).
- [2] K. Kanoda, *J. Phys. Soc. Jpn.* **75**, 051007 (2006).
- [3] I. Bloch, J. Dalibard, and W. Zwerger, *Rev. Mod. Phys.* **80**, 885 (2008).
- [4] For instance, *Frustrated Spin Systems*, ed. H. Diep (World Scientific, Singapore, 2005).
- [5] N. Shannon, O. Sikora, F. Pollmann, K. Penc, and P. Fulde, *Phys. Rev. Lett.* **108**, 067204 (2012).
- [6] B. Normand and Z. Nussinov, *Phys. Rev. Lett.* **112**, 207202 (2014).
- [7] Y. Shimizu, K. Miyagawa, K. Kanoda, M. Maesato, and G. Saito, *Phys. Rev. Lett.* **91**, 107001 (2003).
- [8] T. Itou, A. Oyamada, S. Maegawa, M. Tamura, and R. Kato, *Phys. Rev. B* **77**, 104413 (2008).
- [9] K. Kanoda and R. Kato, *Annu. Rev. Condens. Matter Phys.* **2**, 167 (2011).
- [10] L. Balents, *Nature* **464**, 199 (2010).
- [11] T. Kashima and M. Imada, *J. Phys. Soc. Jpn.* **70**, 3052 (2001).
- [12] T. Mizusaki and M. Imada, *Phys. Rev. B* **74**, 014421 (2006).
- [13] L. F. Tocchio, F. Becca, A. Parola, and S. Sorella, *Phys. Rev. B* **78**, 041101 (2008).
- [14] H.-C. Jiang, H. Yao, and L. Balents, *Phys. Rev. B* **86**, 024424 (2012).
- [15] W.-J. Hu, F. Becca, A. Parola, and S. Sorella, *Phys. Rev. B* **88**, 060402 (2013).
- [16] S.-S. Gong, W. Zhu, D. N. Sheng, O. I. Motrunich, and M. P. A. Fisher, *Phys. Rev. Lett.* **113**, 027201 (2014).
- [17] S. Morita, R. Kaneko, and M. Imada, *J. Phys. Soc. Jpn.* **84**, 024720 (2015).
- [18] S. Sugiura and A. Shimizu, *Phys. Rev. Lett.* **108**, 240401 (2012).
- [19] At the highly frustrated region ($t'/t \sim 0.75$), we also show results for a 18-site ($3\sqrt{2} \times 3\sqrt{2}$) cluster with the anti-periodic boundary condition and a 32-site ($4\sqrt{2} \times 4\sqrt{2}$) cluster of the strong coupling limit with the periodic boundary condition to examine the finite-size effects.
- [20] M. Imada and M. Takahashi, *J. Phys. Soc. Jpn.* **55**, 3354 (1986).
- [21] J. Jaklič and P. Prelovšek, *Phys. Rev. B* **49**, 5065 (1994).
- [22] A. Hams and H. De Raedt, *Phys. Rev. E* **62**, 4365 (2000).
- [23] H. Shiba and P. A. Pincus, *Phys. Rev. B* **5**, 1966 (1972).
- [24] R. M. Fye and R. T. Scalettar, *Phys. Rev. B* **36**, 3833 (1987).
- [25] N. Kawakami, T. Usuki, and A. Okiji, *Physics Letters A* **137**, 287 (1989).
- [26] A. Georges and W. Krauth, *Phys. Rev. B* **48**, 7167 (1993).
- [27] D. Duffy and A. Moreo, *Phys. Rev. B* **55**, 12918 (1997).
- [28] G. Jüttner, A. Klumper, and J. Suzuki, *Nuclear Physics B* **522**, 471 (1998).
- [29] S. Onoda and M. Imada, *Phys. Rev. B* **67**, 161102 (2003).
- [30] M. Laubach, R. Thomale, C. Platt, W. Hanke, and G. Li, *Phys. Rev. B* **91**, 245125 (2015).
- [31] J. P. F. LeBlanc, A. E. Antipov, F. Becca, I. W. Bulik, G. K.-L. Chan, C.-M. Chung, Y. Deng, M. Ferrero, T. M. Henderson, C. A. Jiménez-Hoyos, et al. (Simons Collaboration on the Many-Electron Problem), *Phys. Rev. X* **5**, 041041 (2015).
- [32] K. Takai, K. Ido, T. Misawa, Y. Yamaji, and M. Imada, *J. Phys. Soc. Jpn.* **85**, 034601 (2016).
- [33] H.-Y. Yang, A. M. Läuchli, F. Mila, and K. P. Schmidt, *Phys. Rev. Lett.* **105**, 267204 (2010).
- [34] G. Kotliar, E. Lange, and M. J. Rozenberg, *Phys. Rev. Lett.* **84**, 5180 (2000).
- [35] T. Koretsune, Y. Motome, and A. Furusaki, *J. Phys. Soc. Jpn.* **76**, 074719 (2007).
- [36] M. Imada, *Phys. Rev. B* **72**, 075113 (2005).
- [37] T. Misawa and M. Imada, *Phys. Rev. B* **75**, 115121 (2007).
- [38] T. Misawa, Y. Yamaji, and M. Imada, *J. Phys. Soc. Jpn.* **75**, 083705 (2006).
- [39] H. Morita, S. Watanabe, and M. Imada, *J. Phys. Soc. Jpn.* **71**, 2109 (2002).
- [40] A. Kitaev, *Annals Phys.* **321**, 2 (2006).
- [41] S. Trebst, arXiv:1701.07056.
- [42] Y. Yamaji, T. Suzuki, T. Yamada, S.-i. Suga, N. Kawashima, and M. Imada, *Phys. Rev. B* **93**, 174425 (2016).
- [43] T. Senthil, *Phys. Rev. B* **78**, 035103 (2008).
- [44] R. V. Mishmash, I. González, R. G. Melko, O. I. Motrunich, and M. P. A. Fisher, *Phys. Rev. B* **91**, 235140 (2015).
- [45] P. Sengupta, A. W. Sandvik, and R. R. P. Singh, *Phys. Rev. B* **68**, 094423 (2003).
- [46] K. Watanabe, H. Kawamura, H. Nakano, and T. Sakai, *J. Phys. Soc. Jpn.* **83**, 034714 (2014).
- [47] M. Kawamura, K. Yoshimi, T. Misawa, Y. Yamaji, S. Todo, and N. Kawashima, *Comput. Phys. Commun.* **217**, 180 (2017).
- [48] <http://ma.cms-initiative.jp/en/application-list/hphi>.
- [49] <https://github.com/QLMS/HPhi>.